Bioparticles consisting of olive mill wastewater (OMW)-adapted bacteria and OMW-polluted soil as carrier– An application in an anaerobic fluidized bed bioreactor

M.C. Morón[a,1], L. Pozo-Morales[b,*], D. Garvi[a], A.J. Alonso-Contreras[a], J. Lebrato[a,2]

[a] TAR Group RNM159 PAIDI, University of Seville. 7, Polytechnic School, Virgen de África, st. 41011, Seville, Spain
[b] Department of Chemical Engineering, Polytechnic School, University of Seville, Virgen de África, st., 41011, Seville, Spain

Keywords:

Olive mill wastewater
Soil
Adapted biomass
Anaerobic fluidized bed reactors
Design

A B S T R A C T

The world olive oil production represents a very significant sector of the alimentary industry. Nonetheless, the spillages associated to the sector –olive mill wastewater (OMW)– imply serious environmental risks due to their difficult treatments. This study showcases the use of bioparticles from a soil that has repeatedly been con-taminated by OMW, to treat water also polluted by OMW. The bacterial biomass that develops overtime within a OMW-polluted course becomes adapted to its conditions and proves effective in its treatment. Water and soil samples were taken from a watercourse that has been suffering from periodic OMW discharges during the last 25 years. Two main factors were identified as the causes of the efficiency of these soils as a means of biological treatment: high concentrations and extended adaptation of active biomass to the pollutants present in the wa-tercourse. The start-up times of the biological processes are reduced since no adaptation period is necessary. This makes it possible to eschew pre-treatment procedures in biological processes. A guide for the design of a con-tinuous flow anaerobic fluidized bed bioreactor (AnFBR) is provided. A stream of 300 $m^3 d^{-1}$ and 5000 mg L^{-1} COD generates an electrical and thermal energy of 1654 kW h d^{-1} and 2341 kW h d^{-1} respectively.

1. Introduction

During the year 2017 the world olive oil production went over the 3 million t/year mark, which is to say it saw an increase of almost 30% in comparison to the previous year [1]. The Spanish production accounts for 41% of that of the world.

This brings to light the definite importance of this sector of the food industry, especially taking into account the fact that it is experiencing a steady growth with the Mediterranean region as the leading olive-growing area in the world. Nevertheless, the pollution that is associated with the waste that originates during the olive processing is the origin of great environmental troubles [2–5].

Olive mill wastewater (OMW) is the liquid by-product generated during the production of olive oil. Even though OMW might feature very different characteristics depending on factors such as their region of origin, climate conditions, means of extraction and associated growing and processment methods, it can be generally described as a dark-coloured waste containing great levels of insoluble and soluble organic substances such as lipids, sugars, polyalcohols, amino acids as well as high concentrations of polyphenolic compounds (up to 10 g L^{-1}), [6] which contribute to its elevated organic load (50–200 g L^{-1} COD). Also, its pH values are very low. All of these result in a toxic effect which can change the physicochemical and biological properties of the soil [7] and eventually make its treatment immensely difficult. Furthermore, the BOD/COD ratio of OMW ranges between 0.40 and 0.55, which is below the threshold to be considered a biode-gradable waste according to the literature [8].

The main problem regarding the disposal of OMW is to find an environmentally friendly and economically viable solution. Many re-searchers have proposed treatment methods to reduce its organic load. As an alternative, new ways are being opened such as OMW valorisa-tion thanks its potential as a substrate for bioconversions [9,10].

Despite its low biodegradability, biotreatment is still considered useful in OMW treatments as it is the most economical way to degrade

* Corresponding author at: Virgen de África, st. 41011, Seville, Spain.
E-mail addresses: cmoron@us.es (M.C. Morón), lauratar@us.es (L. Pozo-Morales), mgarvi@us.es (D. Garvi), sedceroya@us.es (A.J. Alonso-Contreras), grupotar@us.es (J. Lebrato).
[1] Department of Applied Physic I.
[2] Polytechnic School.

organic waste. Since anaerobic processes hydrolyzes pollutants with complex structure into simpler compounds which can be degraded *via* aerobic processes, anaerobic processes are particularly suitable for wastewater with high COD or containing toxic chemicals like polyphenols. In spite of that, in OMW treatment the results are not always satisfactory and some kind of pre-treatment (aside from dilution and nutrients/alkalinity adjustments) is generally necessary. Unsaturated fatty acids are the most resistant compound to biodegradation amongst those present in OMW, whereas polyphenols show the strongest inhibiting effect [11]. Moreover, the presence of these biodegradation-resistant unsaturated fatty acids leads to a low pH which increases the inhibitory action of polyphenols. In general, the bacterial biomass in an aqueous medium is unable to carry out the degradation of these compounds.

It should also be taken into consideration that the Industry demands affordable, reliable and short-term treatments. Biological treatments could satisfy these requirements except for the fact that long time spans are required for the development of a sufficient quantity of bacterial mass that is specifically adapted to be effective in the degradation of OMW.

The hypothesis of this work is that soils affected by long-time organic industrial discharges develop an active biomass which is readily adapted to these specific spills. This adapted biomass is very appropriate to improve the treatment of the industrial polluted waters which are discharged into watercourses. It must be considered that supernatant liquids of these soils are populated, although in less amount, by adapted biomass as well. This is a common situation in watercourses affected by industrial organic discharges [12].

Our research group has been working in the study of the adaptive capacity of microorganisms present in waters and soils which have been receptors of continuous OMW discharges during the last years in order to assess whether it is possible to make use of them as a means of biological treatment. In this paper we evaluate the behaviour of these soils as biological support in reactors with aim at improving their efficiency.

In other words, it is our intention to demonstrate the great ability previously polluted soils have for the treatment of OMW, as well as to design a biologic reactor capable of taking advantage of the properties of these soils.

In order to asses to what extent was polluted soil useful, soil and water samples of a real watercourse affected by OMW spillage over a long period of time were taken. The results obtained indicate that the samples that were treated with the aforementioned adapted biomass displayed the highest efficiency.

In order to design a suitable biological reactor for this process, it must be taken into account that these adapted bacteria are mostly anaerobic, as well as the fact that immobilized biomass is commonly used in anaerobic processes due to the higher biomass concentration in comparison to activated sludge processes. Regarding these factors, various anaerobic bioreactors such as upflow anaerobic sludge blanket, expanded granular sludge bed, anaerobic biofilter, and anaerobic fluidized bed reactors (AnFBR) reactors are suitable. Among these reactors, AnFBR has the advantage of having been widely implemented in industrial wastewater treatment infrastructures.

By using small and porous carriers, AnFBR provides a large surface area for biomass growth. Moreover, its biomass concentration is usually 5–10 times higher than that of fixed film or conventional activated sludge reactors. AnFBR also provides efficient mixing during fluidization. This allows an organic loading rate (OLR) as high as 40 kg COD m^{-3} d^{-1} to be treated [14].

There are few studies about the design of AnFBR for industrial effluents and they are particularly scarce regarding OMW effluents. Most studies focus on the effect of operating parameters or on their performance. Others placed their spotlight on the hydrodynamic modelling of an AnFBR [15–17].

Important parameters and their quantification (such as minimum fluidization velocity, phase hold up and amount of biogas produced) have been studied, but only very limited studies exist regarding the design strategy of AnFBR [18]. This design strategy should include carrier and bioparticles selection, hydraulic retention time (HRT), bed expansion and superficial velocity. In most practical cases, the design of industrial AnFBR still relies on the experience of the engineers or by rough estimation based on empirical models. This paper described the design of an AnFBR with adapted bioparticles using the method described by *Denz Z, et al.* [18] as a guideline. Nevertheless, the main difference lies in the fact that the latter introduces a further improvement in the AnFBR by means of using bacteria that is specifically adapted to OMW spills, was collected from affected watercourses and uses soil from this watercourse as supporting material. These bacteria were obtained from regular spill points in the bed of the watercourse. Their support material is also soil from the same course.

The present work had the following specific goals: (i) to find biological treatments for OMW with less pre-treatment requirements, (ii) to evaluate the capacity of long-term OMW-polluted soil as a depurator substrate of the organic matter present in OMW and its performance in a real-life environment (an OMW spillage point in the Alcarayón watercourse in Manzanilla, Spain), (iii) to design a AnFBR containing bioparticles from the watercourse soil as support material as well as adhered bacteria that have adapted to OMW conditions after years of continuous spillage, and finally (iv) to assess to what extent it is possible to energetically exploit the biogas produced in the process with aim at improving the overall energetic efficiency of the system and diminishing CO_2 emissions.

2. Materials and methods

2.1. Materials

2.1.1. p-Coumaric acid (pCA) and its derivate compounds

pCA was chosen in order to be tracked as a pollution indicator and to check the evolution of the studied treatment without interferences [12].

In anaerobic conditions, pCA is fully degraded to p-hydroxybenzoic acid in 3 days, to p-hydroxybenzaldehyde in 4 days and to Hydroquinone and Phenol in 7days [19,20]. Therefore, p-hydroxybenzoic acid, hydroquinone, hydroxybenzaldehyde and Phenol can be considered as representative molecules to be determined when verifying pCA degradation routes [13].

Furthermore, it has been suggested that phenol is initially transformed to benzoate *via* reductive carboxylation [21] possibly by *Desulfotomaculum spp, and Clostridium spp* and then through the benzoyl-CoA pathway producing acetate and hydrogen by *Syntrophus spp*. [22–24].

It has also been also reported that phenol can be degraded *via* n-caproate producing acetate and H_2/CO_2 by members of Methanosaetaceae, Methanomicrobiales and Methanobacteriaceae [22,24].

2.1.2. Water and soil samples

The Alcarayón stream flows into the Guadiamar River (Huelva, Spain). The Alcarayón course is affected by OMW discharges at the point where it enters the city of Manzanilla (Huelva, Spain). Up to this point, it is not contaminated by OMW whatsoever.

Water and soil samples were taken in the clean section of the course and exactly in the point that has been suffering from periodic OMW discharges during the last 25 years.

The sampling was carried out following the conservation, transportation and storage instructions of the Standard Methods for the examination of Water and Wastewater, 160, B and C sections [25].

Sampling points (See Fig. 1):

1 Clean point: first stretch of the Alcarayón, where both water and soil

Fig. 1. Sample points.

are still clean because of the absence of industrial discharges. The samples taken here were named: Clean Soil (S_C) and Clean Water (W_C).

2 Spill point: located just in the direct discharge of the OMW. The samples taken here were named: Polluted Soil (S_P) and Polluted Water (W_P).

2.2. Laboratory methods

2.2.1. HPLC determination in reverse phase with UV detection

An innovative analytical method was used to detect pCA –as well as its derivatives– in samples. This consisted of High Performance Liquid Chromatography in reverse phase using an ultraviolet chromatograph (RP-HPLC-UV) [12].

The systems used in the experience consisted of a Gilson HPLC system (Gilson Medical Electronics, Middleton, WI, USA) and a Dynamax UV-1 absorbance detector (Rainin Instrument, Woburn, MA, USA), set at 280 nm. The chromatograms were monitored with an Apple Macintosh Classic II computer.

Chromatographic separations were achieved using a 15 cm x 4.6 or 4.0 mm i.d. Nucleosil C18 (5 µm, 120 Å) at room temperature, preceded by a pre-column that prevents impurities from entering the system.

A reverse-phase HPLC assay was carried out using an isocratic system with a flow rate of 1 ml/min and a mobile phase of acetonitrile.

The instrumental equipment and material that were employed consisted of 25 µl glass micro-syringes, Eppendorf vessels, HPLC filters with 0.45 µm pore diameter, a centrifugal machine and MILI-Q Plus 50 equipment to produce analytical grade water for critical applications (HPLC) and a HPLC.

The employed reagents include liquid chromatographic eluents, ultra-pure water to prepare the mobile phase, reactive and stock solutions of analyzed compounds as well as standard solutions of pCA, p-hydroxybenzoic acid, p-hydroxybenzaldehyde, hydroquinone and phenol. All chemicals were of analytical grade.

Optimal analysis of the samples demanded two fundamental problems to be solved: In the first place, to achieve a sufficient resolution permitting the observation of the complete separation of the compounds (thus allowing for a correct integration), and in the second place, to define accuracy limits and optimal detection conditions.

Samples preparation: samples were centrifuged at a speed of 400 rpm during 10 min to separate suspended particles. The aqueous phase was filtered through a 0.450 µm filter, labelled and frozen until the HPLC analysis.

2.2.2. Advanced analysis of organic matter: TOC and CT. Combustion-Infrared method

In order to quantify the amount of total organic carbon (TOC) the combustion-infrared method was used. Its accuracy depends on the reduction of the molecular size, being appropriate with samples with TOC ≥ 1 mg L^{-1}. The measure of TOC was obtained by measuring total

carbon (TC) and inorganic carbon (IC) separately. The difference between these two measures determined the TOC value. High temperature analyser TOC Dhormann DC-190, combustion method and infrared rays determination were employed [25].

TC: combustion in a muffle furnace set at 680 °C with a platinum catalyst.

IC: it was transformed into CO_2 in an acidification chamber.

In order to determine the Organic Dissolved Carbon, the samples were centrifuged and filtered through a 0.45 μm filter.

2.2.3. Biodegradability assays. Columns

In order to evaluate the presence of an adapted biomass able to perform a natural biological treatment, not only in soils but also in the supernatant, water/soil columns were set in the laboratory with the river samples taken as explained in 2.1. These were 0.38 m glass columns with a valve at the bottom to regulate the output flow. The sediment was covered with aluminium paper in the outside of the column to protect it from light. Every column was filled with 200 ml of sediment and 1 L of water (1:5 soil to water ratio). Four combinations were taken into consideration: clean soil + clean water (S_C/W_C), polluted soil + clean water (S_P/W_C), clean soil + polluted water (S_C/W_P) and polluted soil + polluted water (S_P/W_P).

500 mg pCA, which represents 329.3 mg L^{-1} of TOC, was inoculated into all columns with the intention to simulate an OMW discharge over environments with different types of biomass. In all cases the pCA degradation was measured at different time intervals. In each interval TOC was measured while pCA degradation was registered through RP-HPLC-UV.

The existence, viability and effectiveness of adapted biomass was tested by comparing the results achieved in different situations (Columns: S_C/W_C, S_C/W_P, S_P/W_C, S_P/W_P, by triplicate).

Bibliography indicates that shaking improves the performance of this kind of treatments, reducing the time necessary to obtain a steady output. In our case, shaking was omitted and thus the experience was extended in time to 72 h.

2.2.4. Analysis

The *in situ* determinations were executed by means of a multi parametric sensor of the portable device WTW©MultiLine P4, equipped with pH sensor (± 0.01), dissolved oxygen (DO) sensor (± 0.5%), electric conductivity sensor (± 1%) and temperature probe (± 0.1 °C).

TC, IC and TOC were measured in the samples of supernatant and leachate of the columns in every assay. In every round of measurements, calibration was done by using standards to determinate TC and IC from 10, 100 and 1000 mg L^{-1}. Two annual analysis campaigns took place, in which samples were taken by triplicate. The results displayed here represent all-time average values.

2.3. Design method for a fluidized bed reactor

The concept of fluidization implies that a fluid must go through a static bed of solid particles at a surface velocity that is sufficient to suspend these particles, causing them to adopt a fluid-like behaviour. This maximizes the surface contact between microorganisms and pollutant agents. If the fluid velocity is too low, it will pass through the empty spaces between solid particles and the bed remains still. On the contrary, at a sufficient velocity, the bed expands until the particles become suspended in the fluid [26]. The minimal fluidization velocity is obtained when the pressure drop through the bed is equal to the weight of the particles. In this scenario, the bed will become completely suspended [27]. The expansion degree of the bed depends on the size and density of the particles as well as on the velocity d of the upward flux and its viscosity.

Design

The design of this AnFBR counts with two sections. One is the reaction section, where bioparticles move upwards inside a draft tube and then circulate downwards once they are outside of it. The other is the separation section, where bioparticles decant in the sedimentation zone prior to returning to the reaction section.

Regarding the geometry of the reactor, it should be noted that [28,29], square-shaped reactors involve a much simpler construction process than cylinder-shaped systems, although they suffer from the disadvantage of a slower mixing due to the existence of still zones. Nevertheless, given the fact that our design includes a draft tube, it is possible use a square shape in this reactor without suffering from this disadvantage. Furthermore, a conic base introduces better performance and hydrodynamic features [30] than a constant cross-section. It has been reported that the angle that led to a best performances is 5° [30] although values ranging from 1 to 5 degrees also work.

Finally, a low (static bed height (H) / reactor diameter (d_r)) dimensional ratio will improve the mixing of both phases, although a higher ratio would provide a wider surface area for the growth of bioparticles. Values between 2 and 5 are recommended [30].

2.3.1. Support material and bioparticles

The support material was soil form the Alcarayón stream containing OMW-adapted bacteria that are responsible for the treatment, both of which constitute the bioparticles. In order for the system to work, these microorganisms must be able to handle OMW treatment with guaranteed performance, absence of leakings, short start-up times and a high adaptive capacity to load variations.

These bioparticles were characterized according to the method explained in Table 1.

2.3.2. Design of the reaction section in the AnFBR

The following parameters are involved in the design of this section: Hydraulic retention time (HRT), OLR, sludge loading rate (SLR), percentage of bioparticles in the reactor, fluidification velocities of the system, sludge discharge frequency, biogas recycling rate and liquid recycling rate [18]. These parameters provide the size of the reactor as well as its optimal operating conditions. In order to design a stable reactor that is able to effectively degrade these pollutants, the following parameters should remain within the ranges described in the bibliography regarding the BOD/COD rate: HRT, OLR, SLR and bioparticle volume [18,14], Table 2.

2.3.3. Determination of the bioparticle discharge frequency (t_d) and the liquid and biogas recycling frequency

During this treatment the biomass will use the pollutant agents as nutrients and grow inside the reactor. Consequently, biomass concentration increases as well as the SLR of the system. If the SLR reaches its lower limit value (Table 2), a bioparticle discharge is needed. The time span between bioparticle discharges t_d can be calculated considering the biomass balance within the reactor, as explained in Table 4.

2.3.4. Determination of the biogas production rate

The biogas produced as a result of the anaerobic process of by COD removal can be used to enhance mixing inside the AnFBR.

2.3.5. Determination of the biogas and liquid recycling rate

Inside the AnFBR, the bioparticles ascend throughout the draft tube and are subsequently recirculated towards the base of the reactor on the outside of the tube. This allows for an efficient mix of bioparticles and wastewater, enhancing organics elimination.

In turn, fluidization relies upon the recirculation of liquid and biogas –the latter of which was produced in the anaerobic process and is repurposed into the mixing and fluidization of bioparticles in order to save energy. The liquid and biogas recycling ratios are defined as the ratio of liquid and biogas recirculation flowrate, respectively, to the influent flowrate. Moreover, liquid and biogas recirculation flowrates need to be determined through experimentation given that they depend

Table 1
Characterization method of support material and bioparticles.

Support materials:	1. Determination of the density of the support material (ρ_s).
Soil from the Alcarayón course	2. Determination of the particle diameter (d_p). Classification according to Geldart [31] and verification that the particle is either in group B or D.
	(*) Suitable for wastewater treatment [31]
	3. Determination of porosity (ε) [32]
	4.Verification of requirements [14]:
	4.1. Good bacterial adhesion.
	4.2. d_p: 0.1–0.7 mm
	4.3. High porosity and specific surface.
	4.4. ρ_s: 1500–2500 kg m^{-3}.
	4.5. Hydrophilic
Bioparticles:	1.In-laboratory assessment of the adapted bacteria as a means of wastewater treatment. The procedures regarding the columns are described in 2.2
Naturally formed biomass from the Alcarayón stream containing OMW-adapted bacteria.	2.Selection of the best bioparticles regarding the results obtained.
Surface velocity [33]	$U_{mf} = \frac{d^2(\rho_s - \rho)g}{1650 \cdot \mu}$
U_f = fluid volumetric flux velocity / reactor cross-section area.	U_{mf} (m h^{-1})
$U_{mf} < U_f < U_t$	d = solid particle diameter (mm)
U_{mf} = Minimal fluidization velocity	ρ_s, ρ_w = specific weight of the solid and the water (g m^{-3})
U_t = terminal fluidification velocity (at which the particles are drawn into the liquid)	μ = water dynamic viscosity (g m^{-1} h^{-1})
	g = gravity (m h^{-2})
Specific area after fluidization	$a_s = \frac{6(1-\square)}{dp\,\psi}$
	a_s = specific surface (m^{-2})
	ε = porosity (%)
	d_p = support particle porosity (mm)
	ψ = form factor (no dimensions, 1 pseudospheric particle)

not only on the pressure drop and fluidization velocities, but also on structural aspects of the reactor, especially those concerning the diffusion plate, which allows the gas to homogeneously dilute into bubbles when it enters the fluid. Since no pilot reactor was constructed in this study, we took into consideration the values described by the literature focused thereon. As a conclusion, we recommend that upon designing an AnFBR, a small liquid recirculation ratio and a larger biogas recirculation ratio should be used. This allows for a lower liquid recirculation rate in the reactor, ranging between 2 and 10 [34]. Then, experimental observations would allow to fine-tune these values accordingly to the particular characteristics of the reactor. In cases where the mixing between bioparticles and wastewater is not effective at a low liquid recirculation ratio, the latter can be increased by rising the biogas recirculation ratio, thus lowering the energy consumption of the reactor.

3. Results and discussion regarding the behaviour of the adapted bacteria

3.1. Physical and chemical parameters

Table 6 displays the results obtained in the characterization of the supernatant in each reactor. The W_C values are representative of natural clean waters without any eutrophication problems. However, DO levels are lower than expected due to a slow river flow. The W_P samples were dark-coloured, with a high electric conductivity and almost free of DO. The dramatic drop in dissolved oxygen is symptomatic of a sudden and pronounced water contamination by a high-salinity, low-pH spillage. These are specific traits to OMW spills.

3.2. Organic matter

Table 7 displays organic matter measurements in supernatant and leachate samples before and after adding pCA over the supernatants. In pCA-free, clean-water supernatant samples, the concentration of pollution in the soil caused the TOC of the aqueous phase to rise due to the dilution of the polluted soil into the water. This evidence supports that significant concentrations of adapted bacteria can indeed be found within the supernatant of a contaminated soil, although they will be adapted to a lesser extent than those found in the soil itself.

As far as supernatants are concerned, the following phenomena are to be described:

When water polluted by the industrial discharge entered the clean soil in column S_C/W_P, the TOC removal rate increased in 21.5% above that obtained in the S_C/W_C column, thanks to the presence of adapted biomass within the sample itself.

In the same manner, TOC removal rate rose when polluted soil was treated, although these values were lower than expected considering the higher amounts of adapted biomass. This suggests that a bigger contact between organic matter and biomass is required. Further investigations on the results when shaking is applied would yield light on this matter. In any case, from an engineering point of view, an AnFBR is the most adequate solution for this requirement due to the fact that they offer the most contact between biomass and the pollutant we are aiming to treat.

The higher performance obtained in the $S_P/W_{P\ column}$ (79.7%) in comparison to the $S_C/W_{C\ column}$ confirms that a biological reactor working with soil with adapted biomass represents, in laboratory scale, a significant increase (63%) in comparison to a liquid-phase reactor with no adapted biomass. Therefore, the behaviour of these soils as

Table 2
Typical values of TRH, OLR, SLR and bioparticle volume percentage in fluidized bed reactors [18][14].

Initial BOD/COD	Maximum affluent COD (mg/L)	SLR (kgCOD/kgVSS d)	OLR (kgCOD/m^3d)	HRT (h)	Percentage of bioparticles in the reactor
≤0.3	≤1500	0.05–0.3	< 3.0	> 12	5–20
0.3–0.5	≤2000	0.1–0.55	1–8	8–48	5–20
> 0.5	≤15000	0,6–2	5–40	3–24	5–20

The design procedures are described in Table 3.

biological support in reactors improves their efficiency. The increase in performance given the same working time (72 h) indicates that the inhibitory effect of polyphenols was reduced in presence of contaminated soils. The development of a sufficient quantity of bacterial mass that is specifically adapted to be effective in degradation of OMW is thus demonstrated.

Throughout the study of the leachate it was observed that the only system without adapted biomass (S_C/W_C) did not only did not present any significant performance, but also accumulated all water-soluble pCA coming from the soil. Before the 72 h running-time of the assay, the leachate reached the value of 505 mg L^{-1} of organic carbon.

The S_C/W_P column treated water merely by means of the active biomass contained in the polluted water. This biomass naturally invaded the soil and adapted to it, leading to a performance of 46.3%. In all cases these values were higher than in the previous column (S_c/W_c).

The performance in TOC removal of the $S_P/W_{C\ column}$ was similar to that of S_C/W_P, despite the lack of movement of the active soil biomass. Although a significant amount of active biomass -higher than in the S_C/W_P- was present in the system, the absence of contact decreased its effectiveness.

The best performance was obtained in the S_P/W_P column, where the greatest amount of active biomass was present both in the mobile (supernatant) and fixed (soil) phases. This performance was of 79.1%.

If the S_P/W_P column is compared to the S_C/W_P, the former shows a more optimal behaviour. S_P/W_P achieved 40% more of TOC removal than S_C/W_P. The behaviour of the latter could be described as that of a conventional reactor without fixed biomass. This proves that, given equal conditions for both reactors, the introduction of polluted soil in one of them improves very significantly its performance.

3.3. Determination of the pCA degradation by RP-HPLC-UV analytical method

From a qualitative point of view, the results of the RP-HPLC-UV analysis were highly congruent with the TOC measurements. In S_c/W_c samples the obtained chromatograms indicated high concentration of pCA in the supernatant. No important amounts of its oxidation derivates were detected (Fig. 2). Nevertheless the chromatograms of the S_c/W_p and S_p/W_c samples were very similar to each other, with lower values of pCA indicating that degradation had begun but not finished. Also p-Hydroxybenzoic acid (route b) and hydroxybenzaldehyde (routes a and c) were detected in similar amounts (Fig. 3). Finally, no significant amounts of pCA and p-hidroxibenzoic acid were detected in W_P/S_P (Fig. 3) indicating that legally-required levels of depuration had almost been reached.

These results indicate that, given the same conditions, the column which had the biggest amount of adapted bacteria from long-time OMW-polluted water and soil was able to remove the whole amount of pCA.

Therefore, we can affirm that the experiments demonstrate that the exploitation of polluted soil opens a new way to achieve an unparalleled performance in adapted biomass OMW treatment with no

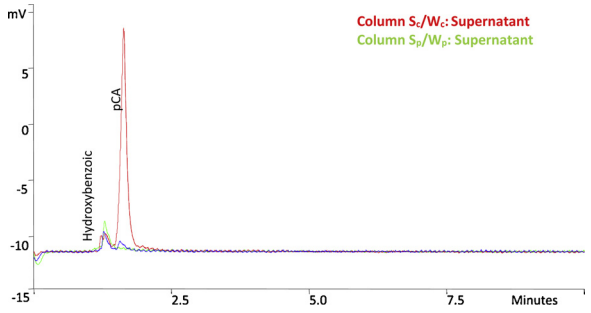

Fig. 2. Chromatograms of supernatant in the S_C/W_C and S_p/W_p samples.

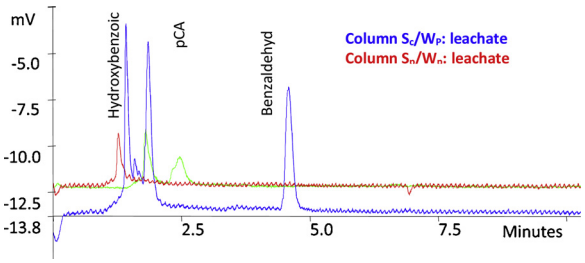

Fig. 3. Chromatograms of leachate in S_C/W_p and S_p/W_p samples.

biological pretreatments.

Throughout the essays (which were carried out in a fixed bed) the ample capacity of the soils to transfer biomass to the supernatant water was observed. Considering that a higher contact between pollutant and specifically adapted biomass would yield a higher effectiveness in treatment, a fluidized bed technology would be the most appropriate. Moreover, the quick spill degradation rate –as observed *via* monitoring of the pCA route– brings a high degree of reliability to this type of treatment. As a result, reactors designed and constructed following these guidelines would be able to substantially optimize treatment times.

4. AnFBR design

The design of a AnFBR for the treatment of OMW is described hereinafter. It relies on the action of bioparticles whose support material is OMW-polluted soil from the Alcarayón watercourse and whose microorganisms are bacteria adapted to this environment.

4.1. Spill characteristics. Initial data

Table 8 includes the features of the spill subject to treatment. A flow of 300 $m^3\ d^{-1}$, similar to that of the actual spill, was considered (Table 9).

4.2. Characterization of the support material and bioparticles

The features of the soil from the Alcarayón course are displayed in Table 10.

Once the percentage of each component has been stablished (Q (0–10)), the bioparticle diameter can be determined taking into account the diameter of medium-grain sand (0,2 mm), silt (0.02 mm) and clay (0.002 mm) particles [36,37]:

$$Ø = 52.15\mu m$$

Given this value, the particle can be classified in Group B [31] according to Geldart:

$$40\ \mu m < Ø < 500\mu m$$

Given the densities of these soil components [38] and considering the aforementioned percentages, bioparticle density can be calculated:

Wet clay: 1760 kg m^{-3}

Sand: 1600–1430 kg m^{-3}

Taking into consideration the percentages from Table 4, it can be established that:

$\rho = 1724.96$ kg m^{-3}

A bioparticle diameter of 52.15 μm and a density of $\rho = 1724{,}96$ kg m^{-3} are considered.

Porosity calculations were carried out using the values displayed in Table 11.

average values are considered in order to calculate porosity:

$$\square(\%) = 43.69$$

The specific surface area of the bed after fluidization will be equal to

Table 3
AnFBR design procedure.

1	Determination of the starting point and the treatment and performance objectives.	BOD/COD rate in the OMW COD ($mg\,L^{-1}$) OMW flow ($m^3\,d^{-1}$)
2	Verification that the OMW COD lies within the values described registered in Table 2.	2000 < COD < 15000 ppm
3	Selection of the HRT value regarding the BOD/COD rate (Table 2)	HRT : 3–24 h
4	Calculations of volume: Total volume (V) Bioparticle volume (VS) (5-20% V) Liquid volume in the reaction section (VL). Maximum amount of biomass per unit volume of bioparticles (Mmax)	HRT = Q / V_L Q = Flow (m^3/h), HRT (h); V_L (m^3) $V = V_L + V_S$ ($V < 700\,m^3$ [34]) $V_S M_{max} = M\,(V_L + V_S)$ [34]
5	OLR calculations. Verification that values are within the range described in Table 2. If else, it should be carried out an iterative calculation with a different HRT as a starting point. This HRT should satisfy the requirements described in point 3.	$OLR = \frac{Q_0 S_0}{V_L + V_S}$ OLR: 5-40 $kg\,COD\,m^{-3}\,d^{-1}$
6	Determination of SLR regarding Table 3 values.	SLR: 0.6 – 2 kg COD $kgVSS^{-1}\,d^{-1}$
7	Calculation of the biomass concentration M.	$M = \frac{OLR}{SLR}$ kg VSS m^{-3}
8	Calculation of M_{max}	$M_{máx}$ point 4 equation.
9	Determination of the reactor geometry: The reactor dimensions are determined by the height (H), length (L_R) and width (W) of a square-shaped reactor.	H/L_R = 0.5–2.5 [34]. L_R/W = 0.8–1.4 [34].

(Table 1):

$$a_s = \frac{6(1-\square)}{dp\,\psi} = 64781.59\,m^{-1}$$

The minimal fluidization velocity is calculated by making use of its corresponding equation (Table 1) at 25 °C.

$$U_{mf} = \frac{d^2(\rho_s - \rho)g}{1650\,\mu} = 13.2\,m\,s^{-1}$$

4.3. Determinations of volume

For an HRT of 14 h, (Tables 3. Point 3 and 4), the following values are true

$V_L = 175\,m^3$

Considering a bioparticle percentage within el reactor of 13% (Table 3 Point 4):

$V_T = V_L + V_S = 201{,}15\,m^3$

$V_s = 26.15\,m^3$

Due to the high reliability of the adapted bacteria, a very low safety factor (10%) was included in the calculations.

$V_T = 221{,}27\,m^3$

OLR value (Point 5, Table 3) = 6.78 $kg\,COD\,m^{-3}\,d^{-1}$

4.4. Calculations of the reactor dimensions

Taking into account the guidelines described in Point 9, the following rate was used: H/L_R = 2,2 y L_R/W = 1,2. Therefore:

L = 4.94 m. Consequently : H= 10.87 m W= 4.12 m

Accordingly, the reactor will have a rectangular shape with a height of 10.87 m, a width of 4.94 and a length of 4.12 m. The draft tube shall be placed in the centre of the reactor, with a cross-section around 50–70% of the cross section of the reactor as well as a height of 75–95% that of the reactor.

4.5. Calculations of the X and x_{max} biomass

According to the calculation procedures from Points 7 and 8 in Table 3:

X = 5.60 kg SSV m^{-3}

$$OLR = \frac{S_0}{TRH\left(\frac{X_{max}}{X_{max}-X}\right)}\;;\; X_{max} = 26.66\,kg\,SSV/m^3$$

4.6. Determination of the discharge rate and the produced biomass per day

Taking into consideration the minimal SLR from Table 2 (with a value of 0.6), step 3 from Table 4 should be applied.

t= t_d, $X = \frac{Q_0 S_0}{SLR_D V}$; X_{dis} = 11.30 kg SSV m^{-3}

With a specific growth rate of $\mu = 0{,}045 d^{-1}$

$$t_d = \frac{\ln\left(\frac{SLR_i}{SLR_D}\right)}{\mu - k_d} = 155.26\,d^{-1}$$

Applying step 2 from Table 5: m_t = 14.53 kg SSV d^{-1}

Table 4
Biomass balance and discharge rate calculations.

1	Biomass balance within the reactor For t = 0, X= X_i For $t = t_d$, $X = \frac{Q_0 S_0}{SLR_d V}$ X_i = initial biomass concentration SLR_d = SLR at the discharge point.	$\frac{dX}{dt} = (\mu - k_d)X.$ dX/dt = biomass variation over a specific timespan μ = specific growth rate (d^{-1}) k_d = specific dead rate (0.01 – 0.06 d^{-1})
2	Calculation of μ	$\mu = \frac{ln\left(\frac{SLR_i}{SLR_d}\right)}{t_2 - t_1}$ X_1 and X_2 = biomass concentration obtained from the linear regression of the data collected in t_1 and t_2, respectively.
3	t_d calculations *via* integration of the equation described in point 1 (Table 4)	$t_d = \frac{ln\left(\frac{SLR_i}{SLR_d}\right)}{\mu - k_d}$

Table 5
CH_4 production and m_t calculations.

1	The produced biogas contains a 65% of CH_4	$G_{methane} = 0.35\,(Q_0(S_0 - S) - 1.42\,m_t)$ (13)
2	Calculations of m_t	m_t = produced biomass per day $m_t = \frac{Q_0 S_0}{t_d}\left(\frac{1}{SLR_d} - \frac{1}{SLR_l}\right)$

Table 6
: Parameters measured *in situ* in water samples.

Parameter	W_c	W_p
DO (mg L^{-1})	4.20	0.27
Electrical Conductivity (mS cm^{-1})	1.16	3.06
pH	7.76	6.90
Temperature (°C)	24.0	28.0

4.7. Cogeneration

The produced biogas (a 54% of which is methane) can be energetically exploited by means of cogeneration equipment as it is available in the market. This generated electricity can be consumed at the same plant, while the heat can be used to keep the reactor at its operating temperature of 25 °C.

Applying step 1 from Table 5: $G_{methane} = 465.27\ m^3\ d^{-1}$; $G_{biogas} = 715.8\ m^3\ d^{-1}$

In order to calculate the expectable volume of generated energy as well as the size of the cogeneration equipment, the amount of produced biogas (715 m^3/day) should be taken into consideration.

Taking into account the technical specifications of the cogeneration engines that are available in the market, the thermal and electrical energy that would be obtained from the cogeneration can be calculated.

Considering the lower heating value and daily production of biogas as well as the thermal and electrical performance of the engines (6.23 kW h m^3), 2341.20 kW h d^{-1} of thermal energy and 1654.45 kW h d^{-1} of electrical energy can be obtained.

Experimental reactors of similar dimensions to the design presented in this study worked at a liquid recirculation ratio of 5.8 and a biogas recirculation ratio of 4.8.

Finally, we include a table summarising the main parameters that characterise the designed AnFBR (Table 12).

Table 8
Initial data regarding the reactor design: spill characteristics.

Flow ($m^3\ d^{-1}$)	300
Main pollutant agent	polyphenolic compounds (PC)
COD (mg L^{-1})	5000
BOD/COD rate	0.55
Temperature (°)	25
pH	6–7
COD removal objective (%)	85

5. Effects of the operational parameters in the designed reactor

The design of the AnFBR is hereby described, although the reactor was not constructed, which could have allowed a further insight and assessment of its behaviour. Nevertheless the following appreciations should be considered:

The parameters that have an effect over the performance of the reactor are pH, temperature, HRT and OLR.

pH has an important influence on microorganisms. A pH that is too high or too low can affect the performance of the reactor due to its inhibiting effect on the intracellular enzymes of the bacteria. The optimal pH for the decay process lies between 6 and 7.

Temperature is especially important in fluidized bed reactors. Nonetheless, unlike in other technologies (such as in fixed bed systems) temperature fluctuations are uncommon in FBR because of their excellent phase mixing.

OLR and SLR values determine respectively the amount of organic components and biomass in the reactor. If they exceed the recommended values a decrease in organic matter removal performance should be expected.

HRT and OLR values are dependent on one another, therefore a

Table 7
TOC evolution.

Reactors	Supernatant (Input, mg L^{-1})				Leachate (Output, mg L^{-1})	
	$TOC_{T=0}$	TOC + pCA*	$TOC_{T=72\,h}$	$TOC_{removal}$(%)	$TOC_{T=72\,h}$	$TOC_{removal}$(%)
S_C/W_c	30.6	359.9	184	48.9	505	0
S_C/W_P	46.9	376.2	153	59.4	202	46.3
S_P/W_c	40.7	370.0	175	52.8	200	45.9
S_P/W_P	53.9	383.2	77.4	79.7	80	79.1

Reactors		Supernatant: water from the course (ppm)				Leachate (ppm)	
		TOC Initial	TOC Initial + 329.3 coumaric acid 0 h	TOC Supernatant 72 h	% $TOC_{removal\ performance}$	TOC 72 h	% $TOC_{removal\ performance}$
Column 1	Clean soil (S_C)/ Clean water (W_C) (*Soil from the Manzanilla course/Water from the Manzanilla course*)	30.6	359.9	184	48.9	505	Supersaturation
Column 2	Clean soil (S_L)/ Polluted water (A_C) (*Soil from the Manzanilla course/Water from the Pilas course*)	46.9	376.2	153	59.4	202	46.3
Column 3	Polluted soil (S_C)/ Clean water (A_L) (*Soil from the Pilas course/Water from the Manzanilla course*)	40.7	370.0	175	52.8	200	45.9
Column 4	Polluted soil (S_C)/ Polluted water (A_C). (*Soil from the Pilas course/Water from the Pilas course*)	53.9	383.2	77.4	79.7	80	79.1

(*) [pCA] = 329.3 mg L^{-1}.

Table 9
Regarding the selection of design parameter values.

COD mg L^{-1}	BOD/COD	SLR (kgCOD kg^{-1} VSS d^{-1})	OLR (kgCOD m^{-3} d^{-1})	HRT (h)	% bioparticles
5000	0.55	1.2	5–40	14	13

Table 10
Characterization of the Alcarayón course [35].

Sectors	Average sand (%)	Silt (%)	Clay (%)
Q (T)	1.2	81.9	16.9
Q (0-10)	21.9	37.7	40.4
Q (10-30)	19.4	45.1	35.5

Table 11
Estimate porosity values (%) [32].

Clays	40 to 60
Silts	35 to 50
fine-grain sand, silty sands	20 to 50

Table 12
Specifications of the fluidized bed reactor.

Affluent flow, Q_0	300 m^3/d
Hydraulic retention time (HTR)	15.4 h
Organic loading Rate (OLR)	6.16 kg COD/m^3d
Sludge load (SLR)	1.1 kg COD/ kg SSV/d
percentage of bioparticle volume	13%
Volume of the reaction region (V)	221.27 m^3
No. of reactors (N)	1
Reactor height (H)	10.87 m
Length of the reaction region (L_R)	4.94 m
Reactor width (W)	4.12 m
bioparticle discharge time (t_d)	155.26 d^{-1}
Biogas production	715.8 m^3/d
Cogeneration: thermal energy	2341.20 kW h/d
Cogeneration: electrical energy	1654.45 kW h/d

change in either one or both of them will affect the performance of the reactor. HRT and OLR values can be manipulated by altering the flow of the system. Given constant OLR values an increase of HRT causes a rise in the performance of the process, up to the point in which HRT exceeds its optimal value, in which case performance will remain constant. When OLR increases, the system performance decreases until the microorganisms adapt to the new system conditions and the system recovers its normal performance. When the substrate is a limiting factor in the process, an increase in OLR can improve the performance of the treatment by feeding the microorganisms and thus generating a further biomass production.

Regarding to what extent the introduction of bioparticles improved the performance of the AnFBR, it is of special interest the experiments carried out with water and soil columns (Section 2.1), predominantly in the W_P/S_C and W_P/S_P columns.

Hereinafter we compare the behaviour of the columns to fixed bed reactors. The W_P/S_C column is comparable to a fixed bed reactor whose biomass were devoid of OMW-adapted bacteria and that received an OMW discharge. In contrast, the W_P/S_P column did have a bacterial population adapted to the OMW spill.

The increase in performance that the adapted bacteria present in the soil introduced was of 20.3% (W_P/S_P *vs* W_P/S_C). Moreover, it should be pointed out that it is known that fluidized bed reactors have a superior performance to fixed bed reactors. Therefore it is expectable an increase in performance of at least 20% in comparison to other AnFBR.

This increase in performance also translates into shorter HRT as well as reactor designs that are sized and operated for higher OLR. Additionally, the system has a high reliability against load variations and eliminates the need for pre-treatment procedures.

6. Conclusions

This work elucidates the important role that long-time OMW-affected soil plays in the degradation of pCA. The efficiency of the soil in the treatment of OMW is hereby demonstrated with an increase of the process performance in no less than a 63% in those columns with soil biomass adapted to industrial pollution. Leachates from columns with adapted biomass in both soil and water faced pCA addition with a performance 79.1% above that of systems based on clean water and soil.

We would like to emphasize that the role of the supernatant characteristics in the degradation of pCA is only second in importance to that of the soil.

pCA degradation by-products -such as p-hidroxybenzoic and hydroxybenzaldehyde- were found in the supernatant and effluent. Their presence is indebted to microorganisms present in the polluted zone, inhabiting both water and soil –a major part of their population is adapted to the presence of polyphenols and possesses the ability to degrade them. Species from water and soils that are free of industrial pollution do not have the enzymatic system that is necessary for this degradation.

The availability of active biomass from the first moment in contaminated soil reduces the start-up times of the biological processes, since no adaptation periods are necessary.

Furthermore, the design of a FBBR is described with regard to the theory, experimentation and knowledge base of these reactors for the treatment of OMW. This design can be described as innovative since there exists no bibliography containing design guidelines for a reactor that makes use of adapted bioparticles.

The biogas that is obtained in the process can be exploited in cogeneration engines with an electrical energy production of 1654.45 kW h d^{-1} and a thermal energy production of 2341.20 kW h d^{-1} given a flow of 300 m^3 day^{-1}.

Moreover, this design allows to set the foundations for the implementation of this reactor as well as similar systems. The exploitation parameters that shall be obtained when taking this design to a full-scale situation will make it possible to verify the assumptions regarding treatment that were described in the beginning of this paper. Additionally, this design includes the usual advantages of anaerobic, fixed bed reactors, as well as it introduces improvements such as the use of adapted bacteria, which will prevent the usual problems associated with these systems.

Funding sources

This research did not receive any specific grant from funding agencies in the public, commercial, or not-for-profit sectors. The funds that have support this research came from the research group, Group TAR University of Seville which carried it out.

Declaration of Competing Interest

The authors declare that they have no known competing financial interests or personal relationships that could have appeared to influence the work reported in this paper. There is no conflict of interest.

References

[1] MAPAMA (Ministerio de agricultura y pesca alimentacion y medio ambiente. Gobierno de España), El Mercado Del Aceite De Oliva Con Una Producción De 1. 229.200 Toneladas Se Sitúa Ligeramente Por Encima De Las Estimaciones Iniciales, (2018), pp. 1–4 Last access July 31st 2018 https://www.mapama.gob.es.

[2] D. Danellakis, I. Ntaikou, M. Kornaros, S. Dailianis, Olive oil mill wastewater toxicity in the marine environment: alterations of stress indices in tissues of mussel Mytilus galloprovincialis, Aquat. Toxicol. 101 (2011) 358–366, https://doi.org/10.1016/j.aquatox.2010.11.015.

[3] G. Hodaifa, M.E. Martínez, S. Sánchez, Use of industrial wastewater from olive-oil extraction for biomass production of Scenedesmus obliquus, Bioresour. Technol. 99 (2008) 1111–1117, https://doi.org/10.1016/j.biortech.2007.02.020.

[4] I. Karaouzas, N.T. Skoulikidis, U. Giannakou, T.A. Albanis, Spatial and temporal effects of olive mill wastewaters to stream macroinvertebrates and aquatic ecosystems status, Water Res. 45 (2011) 6334–6346, https://doi.org/10.1016/j.watres.2011.09.014.

[5] S. Ntougias, F. Gaitis, P. Katsaris, S. Skoulika, N. Iliopoulos, G.I. Zervakis, The effects of olives harvest period and production year on olive mill wastewater properties – evaluation of Pleurotus strains as bioindicators of the effluent's toxicity, Chemosphere 92 (2013) 399–405, https://doi.org/10.1016/j.chemosphere.2013.01.033.

[6] S. Campanari, F. Augelletti, S. Rossetti, F. Sciubba, M. Villano, M. Majone, Enhancing a multi-stage process for olive oil mill wastewater valorization towards polyhydroxyalkanoates and biogas production, Chem. Eng. J. 317 (2017) 280–289, https://doi.org/10.1016/j.cej.2017.02.094.

[7] A. Mekki, A. Dhouib, S. Sayadi, Evolution of several soil properties following amendment with olive mill wastewater, Prog. Nat. Sci. 19 (2009) 1515–1521, https://doi.org/10.1016/j.pnsc.2009.04.014.

[8] J.T. Novak, S. Banjade, S.N. Murthy, Combined anaerobic and aerobic digestion for increased solids reduction and nitrogen removal, Water Res. 45 (2011) 618–624, https://doi.org/10.1016/j.watres.2010.08.014.

[9] P. Paraskeva, E. Diamadopoulos, Technologies for olive mill wastewater (OMW) treatment : a review, J. Chem. Technol. Biotechnol. 81 (2006), https://doi.org/10.1002/jctb.

[10] J.M. Ochando-pulido, S. Pimentel-moral, V. Verardo, A. Martinez-ferez, A focus on advanced physico-chemical processes for olive mill wastewater treatment, Sep. Purif. Technol. 179 (2017) 161–174, https://doi.org/10.1016/j.seppur.2017.02.004.

[11] M. Beccari, M. Majone, L. Torrisi, Two-reactor system with partial phase separation for anaerobic treatment of olive oil mill effluents, Water Sci. Technol. 38 (1998) 53–60, https://doi.org/10.1016/S0273-1223(98)00497-1.

[12] M.C. Morón, L. Pozo-Morales, C. Benito Mora, D. Garvi, J. Lebrato, OMW spillage control tool based on tracking p-Coumaric acid degradation by HPLC, Environ. Technol. (United Kingdom) (2018), https://doi.org/10.1080/09593330.2018.1439108.

[13] K. Pei, J. Ou, J. Huang, S. Ou, p-Coumaric acid and its conjugates: dietary sources, pharmacokinetic properties and biological activities, J. Sci. Food Agric. (2016), https://doi.org/10.1002/jsfa.7578.

[14] J.J. Heijnen, A. Mulder, W. Enger, F. Hoeks, Review on the application of anaerobic fluidized bed reactors in waste-water treatment, Chem. Eng. J. 41 (1989) 37–50, https://doi.org/10.1016/0300-9467(89)80029-2.

[15] M. Fuentes, N.J. Scenna, P.A. Aguirre, M.C. Mussati, Hydrodynamic aspects in anaerobic fluidized bed reactor modeling, Chem. Eng. Process Process Intensif. 47 (2008) 1530–1540, https://doi.org/10.1016/j.cep.2007.07.001.

[16] C.S. Wu, J.S. Huang, R. Ohara, Hydrodynamics of tapered anaerobic fluidized beds for metabolic gas production, Chem. Eng. J. 148 (2009) 279–289, https://doi.org/10.1016/j.cej.2008.08.030.

[17] C.S. Wu, J.S. Huang, H.H. Chou, Influence of internal biogas production on hydrodynamic behavior of anaerobic fluidized-bed reactors, Water Res. 40 (2006) 126–136, https://doi.org/10.1016/j.watres.2005.10.036.

[18] Z. Deng, K.Y. Fung, K.M. Ng, C. Wei, Design of anaerobic fluidized bed bioreactor – dyeing effluents, Chem. Eng. Sci. 139 (2016) 273–284, https://doi.org/10.1016/J.CES.2015.09.029.

[19] E. Otal, C. Arnaiz, J.C. Gutierrez, J. Lebrato, Anaerobic degradation of p-coumaric acid and pre-ozonated synthetic water containing this compound, Biochem. Eng. J. 20 (2004) 29–34, https://doi.org/10.1016/j.bej.2004.04.002.

[20] E. Otal, Tratamiento Integrado Químico-biológico De Compuestos Dificilmente Biodegradables, (1998).

[21] T. Kobayashi, T. Hashinaga, E. Mikami, T. Suzuki, et al., Methanogenic degradation of phenol and benzoate in acclimated sludges, in: L. Lijklema, K.R. Imhoff, K.J. Ives, D. Jenkins, R.G. Ludwig, M. Suzuki (Eds.), Pergamon, 1988, pp. 55–65, , https://doi.org/10.1016/B978-1-4832-8439-2.50010-9.

[22] H.H.P. Fang, Y. Liu, S.Z. Ke, T. Zhang, Anaerobic degradation of phenol in wastewater at ambient temperature, Water Sci. Technol. 49 (2004) 95–102, https://doi.org/10.2166/wst.2004.0028.

[23] H.H.P. Fang, D.W. Liang, T. Zhang, Y. Liu, Anaerobic treatment of phenol in wastewater under thermophilic condition, Water Res. 40 (2006) 427–434, https://doi.org/10.1016/j.watres.2005.11.025.

[24] T. Zhang, S.Z. Ke, Y. Liu, H.P. Fang, Microbial characteristics of a methanogenic phenol-degrading sludge, Water Sci. Technol. 52 (2005) 73—78, https://doi.org/10.2166/wst.2005.0500.

[25] E.W. Rice, L. Bridgewater, American Public Health Association, American Water Works Association, Water Environment Federation, Standard Methods for the Examination of Water and Wastewater, 22th ed., American Public Health Association, Washington [Etc.], 2012.

[26] S.P. Burghate, N.W. Ingole, Fluidized bed biofilm reactor – a novel wastewater treatment reactor, Int. J. Res. Environ. Sci. Technol. 3 (2013) 145–155.

[27] M.J.H. Khan, M.A. Hussain, Z. Mansourpour, N. Mostoufi, N.M. Ghasem, E.C. Abdullah, CFD simulation of fluidized bed reactors for polyolefin production - a review, J. Ind. Eng. Chem. 20 (2014) 3919–3946, https://doi.org/10.1016/j.jiec.2014.01.044.

[28] H.S. Choi, M.S. Shin, Hydrodynamics study of two different inverse fluidized reactors for the application of wastewater treatment, Korean J. Chem. Eng. 16 (1999) 670–676, https://doi.org/10.1007/BF02708150.

[29] S. Gorji-Kandi, S.M. Alavi-Amleshi, N. Mostoufi, Experimental investigating the effect of bed geometry on solids mixing in fluidized beds, Part Sci Technol. 34 (2016) 127–133, https://doi.org/10.1080/02726351.2015.1054532.

[30] H. Ju-Sheng, Y. Jii-Lian, W. Chun-Sheng, Comparative bioparticle and hydrodynamic characteristics of conventional and tapered anaerobic fluidized-bed bioreactors, J. Chem. Technol. Biotechnol. 75 (2000) 269–278 doi:10.1002/(SICI)1097-4660(200004)75:4 < 269::AID-JCTB214 > 3.0.CO;2-M.

[31] D. Geldart, Types of gas fluidization, Powder Technol. 7 (1973) 285–292, https://doi.org/10.1016/0032-5910(73)80037-3.

[32] L.L. Sanders, A Manual of Field Hydrogeology, (1998) 381.

[33] A. Ochieng, J.O. Odiyo, M. Mutsago, Biological treatment of mixed industrial wastewaters in a fluidised bed reactor, J. Hazard. Mater. 96 (2003) 79–90, https://doi.org/10.1016/s0304-3894(02)00166-8.

[34] C. Wei, T. Zhang, C. Feng, et al., Treatment of food processing wastewater in a full-scale jet biogas internal loop anaerobic fluidized bed reactor, Biodegradation 22 (2011) 347.

[35] M. Simón, I. Ortiz, I. García, E. Fernández, J. Fernández, C. Dorronsoro, et al., Pollution of soils by the toxic spill of a pyrite mine (Aznalcollar, Spain), Sci. Total Environ. 242 (1999) 105–115, https://doi.org/10.1016/S0048-9697(99)00378-2.

[36] German institute for Standarization. DIN 18123 Soil, investigation and testing - Determination of grain-size distribution. Edition 2011-04.

[37] International Organization for Standardization, Geotechnical investigation and testing. Identification, description and classification of rock. Specifics rules for the identification and description of rock material and mass on the basis of mineralogical composition, ISO 14689, Genetic Aspects, Structu. (2017).

[38] K. Sears, J.E. Alleman, L. Barnard, J.A. Oleszkiewicz, Density and activity characterization of activated sludge flocs, J. Environ. Eng. New York (New York) 132 (2006) 1235–1242, https://doi.org/10.1061/(ASCE)0733-9372(2006)132:10(1235).